A SQUID-BASED BEAM CURRENT MONITOR FOR FAIR / CRYRING*

R. Geithner #, Helmholtz-Institut Jena, Germany & Friedrich-Schiller-Universität Jena, Germany
T. Stöhlker, Helmholtz-Institut Jena, Germany & Friedrich-Schiller-Universität Jena, Germany &
Helmholtzzentrum für Schwerionenforschung, Darmstadt, Germany
R. Neubert, P. Seidel, Friedrich-Schiller-Universität Jena, Germany
F. Kurian, H. Reeg, M. Schwickert,
GSI Helmholtzzentrum für Schwerionenforschung, Darmstadt, Germany

Abstract

A SQUID-based beam current monitor was developed for the upcoming FAIR-Project, providing a non-destructive online monitoring of the beam currents in the nA-range. The Cryogenic Current Comparator (CCC) was optimized for lowest possible noise-limited current resolution together with a high system bandwidth. This CCC should be installed in the CRYRING facility, working as a test bench for FAIR. In this contribution we present results of the completed CCC for FAIR/CRYRING and also arrangements that have been done for the installation of the CCC at CRYRING, regarding the cryostat design.

INTRODUCTION

The high energy beam transport lines (HEBT) at FAIR require a non-intercepting, absolute and precise detection of high brightness, high intensity primary ion beams as well as low intensities of rare isotope beams. The expected beam currents in these beam lines are in the range of few nA up to several µA for continuous as well as bunched beams [1]. This requires a detector with a low detection threshold, a high resolution, and as well as high bandwidth from DC to several kHz.

A superconducting pick-up coil and SQUID system are the main components of a Cryogenic Current Comparator. Superconducting pick-up coils allow the detection of DC magnetic fields created by continuous beams without applying modulation techniques. A SQUID acting as current sensor for the pick-up coil enables the detection of lowest currents. Therewith the CCC optimally fulfils the requirements for the FAIR beam parameters.

DESIGN AND WORKING PRINCIPLE

The CCC [2, 3, 4] consists of a meander-shaped niobium shielding, a toroidal niobium pick-up coil with a ferromagnetic core, a toroidal matching transformer also including a ferromagnetic core and an LTS SQUID with the appropriate SQUID-electronics (see Fig. 1).

* Work supported by GSI Helmholtzzentrum für Schwerionenforschung, Darmstadt, Germany and Helmholtz-Institut Jena, Germany

rene.geithner@uni-jena.de

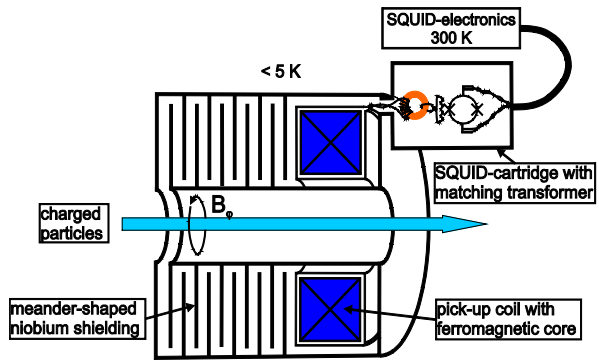

Figure 1: Circuit diagram of the CCC.

The azimuthal magnetic field of the particle beam passes the ceramic gap in the beam line and is guided to the pick-up coil by the meander-shaped shielding whereby all other external magnetic field components are strongly attenuated [3, 5].

Sensitivity Optimization

The total intrinsic noise of the entire CCC is composed by the intrinsic noise of the SQUID itself and its electronics, as well as the magnetization noise of the embedded coils. The spectral current density $\langle I^2 \rangle$ of a coil coupled to the input coil L_I of a SQUID at a temperature T can be calculated with the Fluctuation-Dissipation-Theorem (FDT) and the measured frequency-dependent serial inductance $L_S(\nu)$, respectively. With the serial resistance $R_S(\nu)$ in the equivalent circuit diagram of a real coil, $R_S(\nu)$ represents the total losses [6, 7]:

$$\langle I^2 \rangle = 4k_B T \int \frac{R_S(\nu)}{\left(2\pi\nu\left(L_I + L_S(\nu)\right)\right)^2 + \left(R_S(\nu)\right)^2} \qquad (1)$$

As one can see in Equation (1) the current noise decreases if $L_S(\nu)$ is as high as possible and, secondly, $R_S(\nu)$ remains low over the whole frequency range.

From preliminary investigations [5, 7] we found that the nanocrystalline ferromagnetic material Nanoperm [8] shows very satisfying results matching our requirements. A single-turn Niobium toroidal pick-up coil was electron-beam welded around a Nanoperm M764 core. This pick-up coil has an outer diameter 260 mm, an inner diameter of 205 mm and a width of 97 mm.

A possibility for optimization of the overall current sensitivity of the SQUID detector is the use of a matching transformer with optimized winding ratio and core material.

ISBN 978-3-95450-141-0

For a transformer the current gain in the short-circuit case only depends on the winding ratio, $I_2/I_1 = n_1/n_2$.

However, the CCC with a matching transformer can be described as a series connection of two burdened transformers (see Fig. 2) [4].

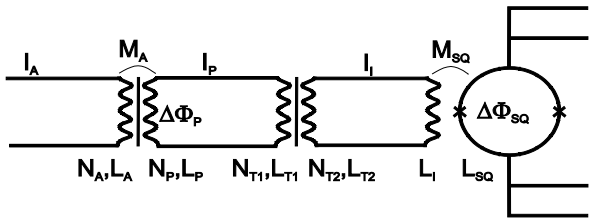

Figure 2: Schematic circuit diagram of the CCC with pick-up coil L_P, matching transformer L_{T1}, L_{T2}, SQUID input coil L_I and SQUID L_{SQ}.

The ratio of the screening currents, I_A, seen by the pick-up coil L_P, and the current through the input coil of the SQUID, I_I, depends on the winding ratio N_{T1}/N_{T2} of the matching transformer, on the inductances L_P of the primary pick-up coil and L_{T1} respectively L_{T2} of the matching transformer, and the input coil of the SQUID, L_I.

$$\frac{I_I}{I_A} = \frac{N_{T1}}{N_{T2}} \cdot \frac{1}{1+\frac{L_I}{L_{T2}}} \cdot \frac{N_A}{N_P} \cdot \frac{1}{1+\frac{L_{T1}L_I}{(L_{T2}+L_I)L_P}} \qquad (2)$$

Setting $N_A = N_P = N_{T2} = 1$, $L_{T1} = N_{T1}^2 \times L_{T2}$, $L_I = 0.46$ µH and $L_P = 103$ µH, I_I/I_A can be plotted as a function of L_{T2} and N_{T1}. There is an optimal number of windings, $N_{T1,\,opt} = 15$, for $L_{T2} = 0.46$ µH where the current gain factor has a maximum of $I_I/I_A = 5.0$. The differences with an unburdened transformer can be seen at this point where the current gain N_{T1}/N_{T2} (= 15/1) should be 15.

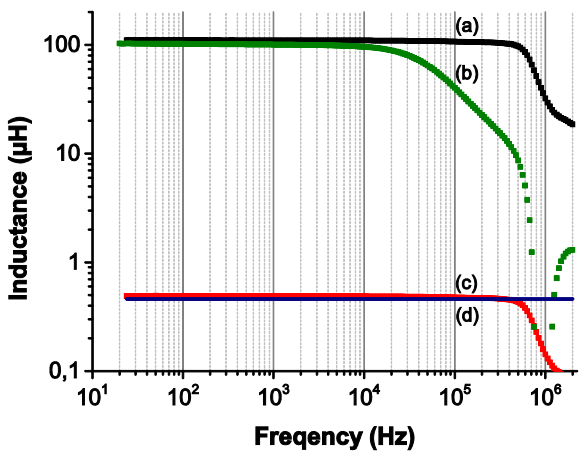

Figure 3: L_S (ν) at 4.2 K for the welded toroidal pick-up coil with Nanoperm M764 core (a), and the primary (b) respectively secondary (c) coil of the matching transformer with Vitrovac 6030 core as well as the SQUID input coil inductance (d).

The dependence on the inductance of the secondary coil of the matching transformer saturates for L_{T2} higher than 0.46 µH which is the inductance of the input coil of the SQUID. Regarding these results the matching transformer was customized by applying 15 turns respectively 1 turn of niobium wire to a selected Vitrovac 6030 [4, 9] core.

Figure 3 shows the frequency dependence L_P (ν) at 4.2 K of the FAIR-CCC's single-turn toroidal pick-up coil with Nanoperm M764 core and the primary L_{T1} (ν) with $N_{T1} = 15$ respective secondary coil L_{T2} (ν) with $N_{T2} = 1$ of the matching transformer with Vitrovac 6030 core. The frequency characteristics of serial inductance L_S (ν) and the serial resistance R_S (ν) of the coils were measured with a commercial Agilent E4980A LCR-Meter [8].

The inductance of the pick-up coil of $L_P = 103$ µH matches quite well to the inductance of the matching transformer's primary coil $L_{T1} = 110$ µH as well as the inductance of the matching transformer's secondary coil $L_{T2} = 0.49$ µH to the inductance of the SQUID input coil of $L_I = 0.46$ µH. Inserting these measured values in Eq. (2) yields an overall current gain factor of 5.1. It could be shown that the inductance of the welded coil with the Nanoperm M764 core is almost constant for frequencies below 10 kHz (see (b) in Fig. 3). L_{T1} respectively L_{T2} (see (b), (c) in Fig. 3) are even constant up to 400 kHz which promises high system bandwidths.

EXPERIMENTAL RESULTS

For the presented results of the completed FAIR-CCC including its matching transformer, a SQUID sensor 'CP2 blue' from the manufacturer Supracon [10] in combination with a 'XFF-1' readout electronics from the manufacturer Magnicon [11] were used.

Step Function Response

Figure 4 shows the response of the completed FAIR-CCC with matching transformer to a rectangular current signal of 2 µA (a), 1 µA (b), 200 nA (c), 100 nA (d), 20 nA (e), and 10 nA (f) applied to a beam simulating wire along the beam axis with the help of a battery powered current source. The response is plotted as the magnetic flux seen by the SQUID in units of the magnetic flux quantum Φ_0 as calculated from the output voltage and the flux sensitivity of the SQUID system. The flux sensitivity was adjusted to 0.103 V/Φ_0 and the bandwidth of the SQUID system to 217 kHz. There is no low pass filter or time averaging used in the output circuit of the CCC. From this curves it is also visible that there is close to zero drift in the CCC signal during a time span of at least 5 s. The smoothing at the rising edge of the signal at higher currents (curve (a)) appears due to the use of a 10 Hz low-pass filter in the input to prevent RF-interferences and is not a characteristic of the CCC.

ISBN 978-3-95450-141-0

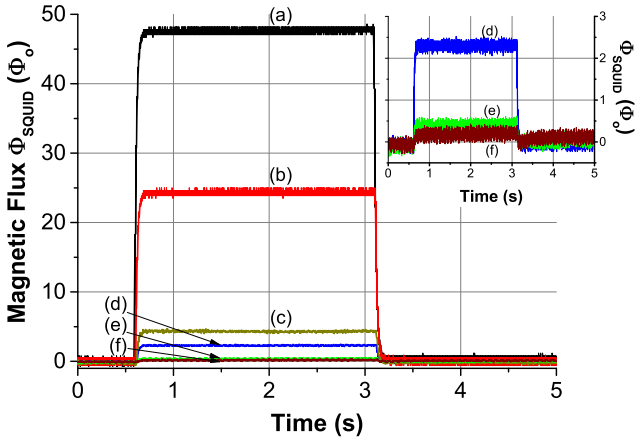

Figure 4: Response of the completed FAIR-CCC with matching transformer to a rectangular current pulse of 2 µA (a), 1 µA (b), 200 nA (c), 100 nA (d), 20 nA (e), and 10 nA (f) applied to a beam simulating wire along the beam axis (insert with magnified scale).

Figure 5 depicts the peak-to-peak value of the step function response in units of the magnetic flux quantum versus the applied calibration current between 10 and 2000 nA, which is linear over the plotted range. This graph displays another advantage of the CCC. Using a simple wire along the beam axis or an additional wire coil around the pick-up coil enables an easy calibration with a linear response. From the responses to the different current pulses an overall current sensitivity of 42 nA/Φ_0 could be calculated. In the case of the direct coupled pick-up coil the current sensitivity was 190 nA/Φ_0. The overall current sensitivity therefore was enhanced by a factor of 4.5 using the matching transformer compared to the direct coupled pick-up coil.

Figure 6 shows the step function response of the CCC to a calibration current of 14 nA with a low slew rate of the applied signal.

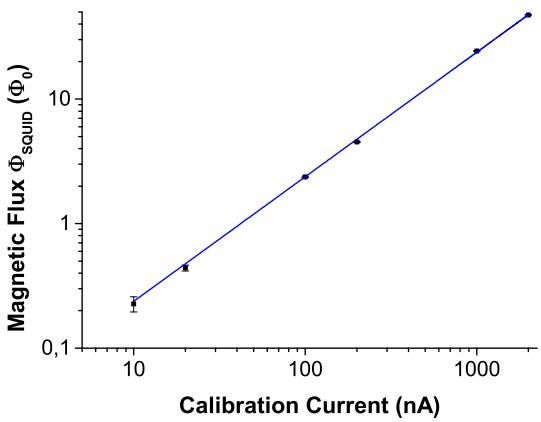

Figure 5: The plot of the peak-to-peak value of the step function response of the completed FAIR-CCC vs. calibration current shows a linear transfer function.

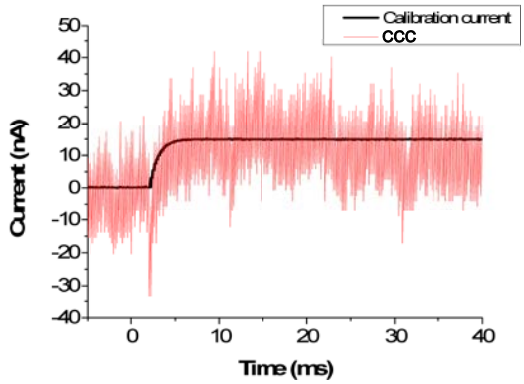

Figure 6: Response of the completed FAIR-CCC with matching transformer (red curve) to a current pulse of 14 nA applied to a beam simulating wire along the beam axis (black curve).

It is shown that the CCC signal follows the calibration current instantaneous and delivers the same amplitude with the calculated overall current sensitivity from Fig. 5. The smoothing at the rising edge of the calibration current is caused by the limited bandwidth of the battery powered current source. When test signals with higher slew rates from a battery powered current source with a higher bandwidth are applied, the slew rate of the signal exceeds the maximum slew rate of the CCC and an overshooting appears (see Fig. 7). For the signals shown in Fig. 7 the SQUID electronics in the FLL-mode is able to stabilize the working point and the peak-to-peak values of the measured CCC signals correspond to the measured current values from the battery powered current source. For signals with higher slew rates it might happen, that the SQUID electronics in the FLL-mode adjusts to another working point and flux jumps in the CCC signal may appear.

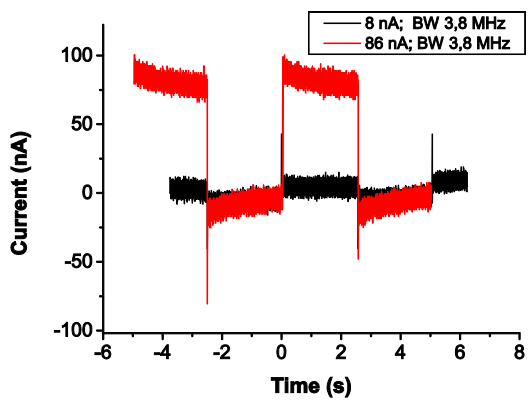

Figure 7: Response of the completed FAIR-CCC with matching transformer to a current pulse of 8 nA (black curve) and 86 nA (red curve) applied to a beam simulating wire along the beam with higher slew rates.

ISBN 978-3-95450-141-0

Noise Measurements

The output voltage noise density of the SQUID electronics was measured by an HP 89410A vector signal analyzer. The current noise density was calculated using the flux and current sensitivity of the setup.

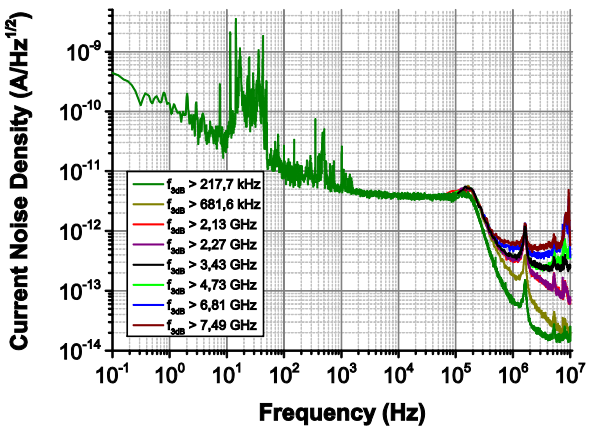

Figure 8: Current noise density of the FAIR-CCC with matching transformer for several SQUID system bandwidths.

Figure 8 shows the measured current noise density of the FAIR-CCC with matching transformer using the Supracon's SQUID sensor CP2 blue and Magnicon's XFF-1 SQUID electronics. The current noise density was measured to be 35 pA/Hz$^{1/2}$ at 7 Hz and to 3,5 pA/Hz$^{1/2}$ at 10 kHz, cf. Fig. 8. The total noise of the completed FAIR-CCC is calculated to be 3 nA in the frequency range from 0.2 Hz to 10 MHz.

Due to the limited bandwidth of the battery powered current source it was not feasible to measure the bandwidth of the CCC directly. Regarding the frequency dependent inductances of the coils in Fig. 3, it turns out that the bandwidth of the CCC will be limited by this behaviour. To estimate the bandwidth, noise measurements with several Gain-Bandwidth-Product settings at the SQUID electronics were performed. The 3dB-bandwidth of the SQUID system varies from 217 kHz to 7.49 GHz. All noise figures have a decrease at 200 kHz in common, thus a CCC bandwidth of 200 kHz is estimated. But this needs to be proved by direct measurements.

There appears an additional noise contribution in the frequency spectrum current from 10 Hz to 1 kHz. These so called microphonic effects are caused by the coupling of mechanical vibration of the underground as well as pressure and temperature variations of the helium bath into the CCC. These interactions are not clarified yet and need further investigations.

The results will be directly implemented into the development of a cryostat with local liquid helium supply in order to reduce microphonic effects by damping of mechanical vibrations and, additionally, a pressure and temperature stabilization.

CONCLUSION AND OUTLOOK

The Cryogenic Current Comparator has shown its capability as a beam intensity monitor for ions as well as electrons [12, 13]. It is shown that the transfer function is linear over a wide measurement range. Using an additional wire along the beam axis or around the pick-up coil, that enables an easy and absolute calibration method. Using Nanoperm M764 material, the current noise density of the pick-up coil was reduced by a factor of 2 to 5 compared to previous installations. Including the matching transformer enhances the overall current sensitivity by a factor of 4.5 without increasing the current noise density. The total current noise in the frequency range from 0.2 Hz to 10 MHz calculated to be 3 nA. Minimizing the additional noise due to the microphonic effects should reduce the total noise further more.

This enables the detection of beam currents below 1 nA with the help of filter techniques which means approximately 10^9 ions/spill of $^{238}U^{28+}$ respectively 28×10^9 protons/ spill for slow extraction with t_{spill} = 5 s. Using fast SQUID systems as well as broadband core materials enables time resolved measurements to explore the spill structure of the beam. The estimated CCC bandwidth is 200 kHz still needs to be verified by direct measurements. Together with the improved resolution the sensitivity to coasting beams qualifies the CCC as a well suited instrument for beam diagnostics at FAIR.

The next steps will be the estimation of the CCC slew-rate to qualify the CCC for beam diagnostics of bunched beams with high slew rates. This CCC prototype should be implemented in the CRYRING as test bench for FAIR. Therefore, a cryostat will be designed and fabricated with special focus on damping of mechanical vibrations and a pressure and temperature stabilization, as well as a local helium supply.

REFERENCES

[1] Conceptual Design Report, Darmstadt, 2000, http://www.gsi.de/GSI-Future/cdr/
[2] I. K. Harvey, Rev. Sci. Instrum. 43 (1972) 11, p 1626.
[3] K. Grohmann, H. D. Hahlbohm, D. Hechtfischer, and H. Lübbig, Cryogenics 16 (1976) 10, pp. 601.
[4] R. Geithner, R. Neubert, W. Vodel, M. Schwickert, H. Reeg, R. von Hahn, and P. Seidel, IEEE Trans. Appl. Supercond. 21 (2011) 3, pp. 444-447.
[5] R. Geithner, W. Vodel, R. Neubert, P. Seidel, F. Kurian, H. Reeg, M. Schwickert, Proc. of IBIC 2013, Oxford, UK, TUPF32, 545, 2013.
[6] H. P. Quach, T. C. P. Chui, Cryogenics 44 (2004) 6, pp. 445.
[7] R. Geithner, D. Heinert, R. Neubert, W. Vodel, P. Seidel, Cryogenics 54 (2013), pp. 16-19.
[8] MAGNETEC GmbH, Industriestrasse 7, D-63505 Langenselbold, Germany.
[9] VACUUMSCHMELZEGmbH & Co. KG, GruenerWeg 37, D-63450 Hanau, Germany.

ISBN 978-3-95450-141-0

[10] Supracon AG, An der Lehmgrube 11, 07751 Jena, Germany.
[11] Magnicon GmbH, Barkhausenweg 11, 22339 Hamburg, Germany.
[12] A. Peters, W. Vodel, H. Koch, R. Neubert, H. Reeg, C. H. Schroeder, AIP Conf. Proc. 451 (1998), pp. 163-180.
[13] R. Geithner, R. Neubert, W. Vodel, P. Seidel, K. Knaack, S. Vilcins, K. Wittenburg, O. Kugeler, and J. Knobloch, Rev. Sci. Instrum. 82 (2011), 013302.

ISBN 978-3-95450-141-0